

ZEEMAN EFFECT AND TEMPERATURE DEPENDENCE OF NQR IN DIETHYLTIN  
DIBROMIDE AND DIIODIDE

Tsutomu OKUDA, Morio HIURA, Ryukei BOKU, Koji YAMADA, and Hiaso NEGITA  
Department of Chemistry, Faculty of Science, Hiroshima University,  
Hiroshima 730

The Zeeman effects have been measured for both  $^{81}\text{Br}$  and  $^{127}\text{I}$  nuclei in diethyltin dihalides and the directions of electric field gradient axes have been determined. The temperature dependences of  $^{127}\text{I}$  NQR lines have shown anomalous features. The results were accounted for in terms of the intermolecular bonding.

The crystals of diethyltin dihalides,  $\text{Et}_2\text{SnX}_2$  ( $\text{X}=\text{Br}$  and  $\text{I}$ ), are orthorhombic and belong to  $\text{C}222_1$  and  $\text{Pbcn}$  in the space group, respectively.<sup>1)</sup> As shown in Fig. 1, the molecules in both compounds form chains by the intermolecular  $\text{Sn}\cdots\text{X}$  interaction called 'secondary bonds'.<sup>2)</sup>  $^{81}\text{Br}$  and  $^{127}\text{I}$  NQR frequencies at liquid nitrogen temperature have been reported by Bryuchova et. al.<sup>3)</sup> In order to investigate the nature of the secondary bonds, we measured the Zeeman effect of  $^{81}\text{Br}$  and  $^{127}\text{I}$  NQR lines using single crystals at room temperature. The temperature dependences of the  $^{127}\text{I}$  lines,  $\nu_1$  ( $1/2 - 3/2$ ) and  $\nu_2$  ( $3/2 - 5/2$ ), were also measured between liquid nitrogen temperature and the melting point,  $44^\circ\text{C}$ .

The single crystals were prepared by the Bridgman method. A superregenerative spectrometer with an oscilloscope display was used for the detection of resonance lines. The Zeeman effect was measured by use of the zero-splitting cone method. The magnetic field was provided by Helmholtz coils with a field strength of about  $2 \times 10^{-2}\text{T}$ .

The observed NQR frequencies are listed in Table 1. From the Laue symmetry of the crystals, four zero-splitting cones are expected in both compounds. In

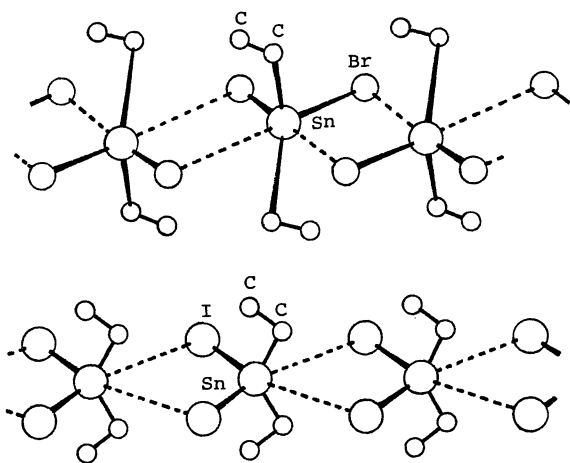


Fig. 1. Structure of  $\text{Et}_2\text{SnX}_2$  ( $\text{X}=\text{Br}$  and  $\text{I}$ ).

the case of  $\text{Et}_2\text{SnBr}_2$ , however, the  $\text{Sn}-\text{Br}$  bonds are nearly parallel to the  $a-c$  plane, so that only two zero-splitting cones were observed within the experimental error. The Zeeman patterns of the  $^{81}\text{Br}$  NQR line are shown in Fig. 2. The orientations of the crystal axes were determined from the symmetry of the observed patterns. Angles between the electric field gradient (efg) axes and the crystal axes determined from the Zeeman studies are compared with the data of X-ray analysis in Table 2.

Table 1.  $^{81}\text{Br}$  and  $^{127}\text{I}$  NQR parameters of  $\text{Et}_2\text{SnX}_2$  (X=Br and I)

compound	Temp/ $^{\circ}\text{C}$	Frequency/MHz		$\eta$	$e^2Qq_{zz}/h^{-1}/\text{MHz}$
		(1/2 - 3/2)	(3/2 - 5/2)		
$\text{Et}_2\text{SnBr}_2$	23	$107.99 \pm 0.01$		$0.132 \pm 0.002^{\text{b}}$	$215.36 \pm 0.04$
	-196	$107.18^{\text{a}}$			
		$112.68^{\text{a}}$			
$\text{Et}_2\text{SnI}_2$	20	$149.60 \pm 0.01$	$295.16 \pm 0.01$	$0.1030 \pm 0.0004^{\text{c}}$	$985.96 \pm 0.08$
	-196	$149.40 \pm 0.01$	$293.30 \pm 0.01$	$0.1206 \pm 0.0004^{\text{c}}$	$980.54 \pm 0.08$

a) Ref. 3.

b) This value was determined by Zeeman effect experiment.

c) These values were determined from the frequency ratio.

It is found from this Table that the efg z-axis lies along the Sn-X bond direction and the y-axis is perpendicular to the Sn-X $\cdots$ Sn plane in both compounds. The x-axis lies nearly along the z-axis of the other bromine atom, i. e. Sn $\cdots$ Br direction, as shown in Fig. 2. The obtained asymmetry parameter ( $\eta$ ) and the nuclear quadrupole coupling constant ( $e^2Qq_{zz}/h$ ) are listed in Table 1. From these parameters the number of electrons in the  $p_x$ ,  $p_y$ , and  $p_z$  orbitals of bromine atom,  $N_x$ ,  $N_y$ , and  $N_z$ , are calculated as Table 3, in which the data of the iodide are also listed.

$N_z$  of the bromide is 1.650 which is larger than that of the iodide, 1.555. Therefore, the ionic character of the Sn-Br bond is larger than that of the Sn-I bond, as expected from the electronegativity consideration. On the other hand,  $(2-N_x)$  is considered to be the number of electrons donated from the halogen atoms to the tin atom. In this case, these electrons form the secondary bond, Sn $\cdots$ X and/or the  $\pi$ -bond, Sn $^- = X^+$ . Furthermore, there is ionic interaction, Sn $^{\delta+} \cdots X^{\delta-}$ , to some extent.

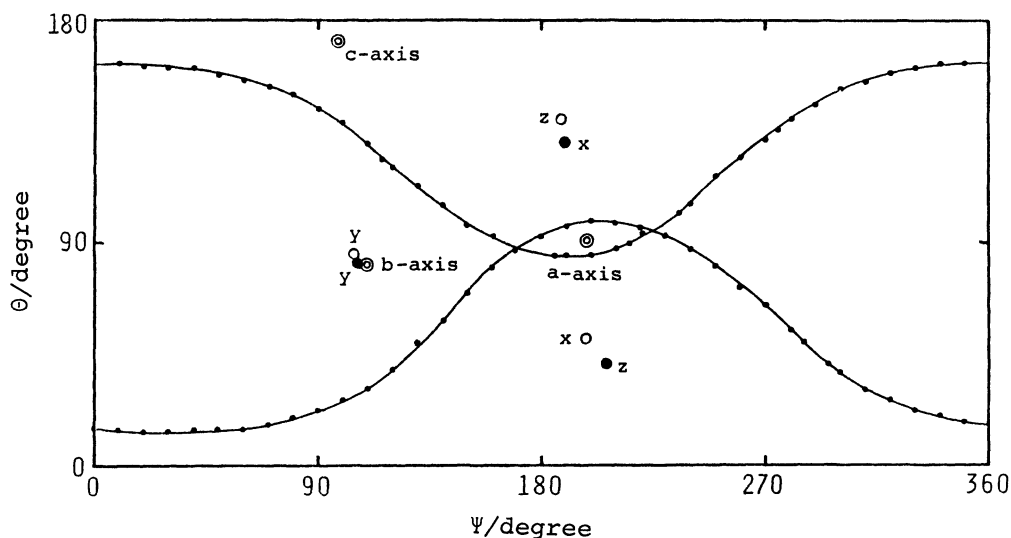


Fig. 2.  $^{81}\text{Br}$  NQR Zeeman patterns of  $\text{Et}_2\text{SnBr}_2$ .

$^{127}\text{I}$  resonance lines in  $\text{Et}_2\text{SnI}_2$  showed anomalous temperature dependences, as seen in Fig. 3. The temperature dependences of the efg tensor components and  $\eta$  were calculated from the frequency ratio, which are shown in Fig. 4. On the basis of the change in the  $N_x$  values in Table 3, we can suggest that the anomalous feature is resulted from the change of the  $\text{Sn}\cdots\text{I}$  secondary bonding character. As the temperature rises, the enhanced thermal vibration will partially destroy the weak  $\text{Sn}\cdots\text{I}$  bond, so that the  $N_x$  value will approach more closely to 2. If this effect overcomes the normal negative temperature dependence,  $|e^2Qq_{zz}/h|$  and  $|e^2Qq_{xx}/h|$  will increase and  $|e^2Qq_{yy}/h|$  decreases with the rise of temperature.

In the case of  $\text{Et}_2\text{SnBr}_2$ , one Br NQR line was observed in accordance with the X-ray analysis at room temperature, while at liquid nitrogen temperature two reso-

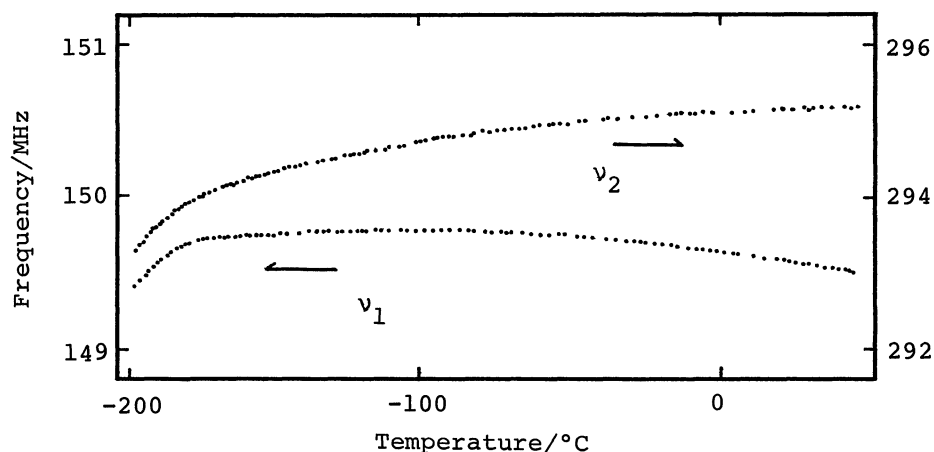


Fig. 3. Temperature dependence of  $^{127}\text{I}$  NQR frequencies in  $\text{Et}_2\text{SnI}_2$ .

Table 2. Angles between the efg axes and the crystal axes (degree)

Compound	efg axis	a-axis	b-axis	c-axis
$\text{Et}_2\text{SnBr}_2$	x	$40.0 \pm 0.2$	$89 \pm 1$	$50.1 \pm 0.1$
	y	$90 \pm 1$ (90.0) <sup>a)</sup>	$3 \pm 1$ (0.0) <sup>a)</sup>	$90 \pm 1$ (90.0) <sup>a)</sup>
	z	$50.1 \pm 0.1$ (49.3) <sup>b)</sup>	$90.7 \pm 0.7$ (90.0) <sup>b)</sup>	$40.0 \pm 0.1$ (40.7) <sup>b)</sup>
$\text{Et}_2\text{SnI}_2$	x	$61 \pm 1$	$70 \pm 1$	$37.4 \pm 0.6$
	y	$53 \pm 1$ (51.4) <sup>a)</sup>	$89 \pm 1$ (90.0) <sup>a)</sup>	$37 \pm 1$ (38.6) <sup>a)</sup>
	z	$51.1 \pm 0.5$ (49.3) <sup>b)</sup>	$53.1 \pm 0.4$ (51.4) <sup>b)</sup>	$60.4 \pm 0.6$ (60.7) <sup>b)</sup>

The values in parentheses were calculated from the X-ray data.

a) The angle between the normal to the X-Sn $\cdots$ X plane and the crystal axes.

b) The angle between the Sn-X bond direction and the crystal axes.

Table 3. p-Orbital populations at halogen atoms

nucleus	Temp./°C	$N_x$	$N_y$	$N_z$
$^{81}\text{Br}$	23	1.970	2	1.650
$^{127}\text{I}$	20	1.970	2	1.555
	-196	1.965	2	1.555

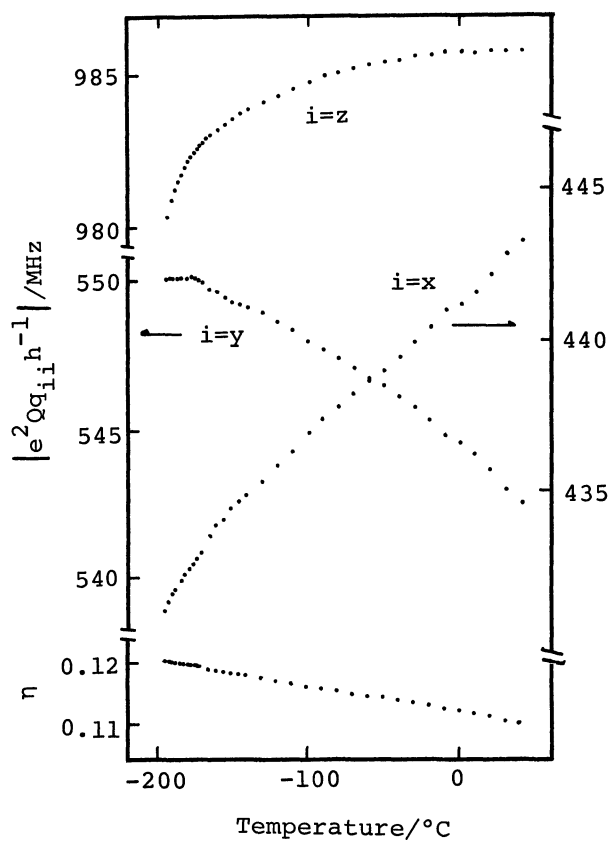


Fig. 4. Temperature dependences of the efg components and  $\eta$  in  $\text{Et}_2\text{SnI}_2$ .

nance lines have been reported.<sup>3)</sup> Consequently, the bromide may undergo phase transition at a temperature between room and liquid nitrogen temperatures.

#### References

- 1) N. W. Alcock and J. F. Sawyer, *J. Chem. Soc. Dalton Trans.*, 1977, 1090.
- 2) N. W. Alcock, *Advan. Inorg. Chem. Radiochem.*, 15, 1 (1972).
- 3) E. V. Bryuchova, G. K. Semin, V. I. Goldanskii, and V. V. Khrapov, *J. Chem. Soc. Chem. Commun.*, 1968, 491.

(Received May 26, 1980)